Categories	Diseases or Functions Annotation	p-value	Predicted Activation State	Activation z-score
Cell Cycle	M phase of tumor cell lines	0.0000	Increased	2.712
	M phase	0.0000	Increased	2.591
	M phase of cervical cancer cell lines	0.0000	Increased	2.126
Immunological Disease	systemic autoimmune syndrome	0.0000	Increased	2.362
Cardiovascular System Development and Function	development of vasculature	0.0000	Increased	2.239
	angiogenesis	0.0000	Increased	2.239
	development of vascular endothelial cells	0.0000	Increased	2.226
	cell movement of endothelial cells	0.0000	Increased	2.171
Cardiovascular Disease	vascular lesion	0.0000	Increased	2.000
Connective Tissue Disorders, Inflammatory Disease, Organismal Injury and Abnormalities, Skeletal and Muscular Disorders	Rheumatic Disease	0.0000	Increased	2.152
Cellular Development, Cellular Growth and Proliferation	cell proliferation of carcinoma cell lines	0.0000	Increased	2.101
Cellular Movement	cell movement of tumor cell lines	0.0000	Increased	2.087

The activation z-score measures the match between expected relationship direction and observed gene expression (≥2 is considered significant).

Supplementary Table S1. Ingenuity Pathway Analysis (IPA) of mouse gene expression in MIR211-overexpressign xenografts compared to A375 parental xenografts.

Gene	A375/211 (Reads)	A375 (Reads)	A375/211 (RPKM)	A375 (RPKM)	logFC (211/A375)	p-value	FDR
Alpl	0.6	43.5	0.2	3.2	-3.7	0.0007	0.01
Amot	15.0	124.0	1.4	3.3	-1.4	0.0179	0.14
Angpt1	9.3	129.2	1.4	5.6	-2.2	0.0006	0.01
Angptl2	201.0	1407.0	38.1	76.0	-1.2	0.0118	0.10
Ankrd44	36.0	239.0	3.8	7.2	-1.1	0.0362	0.22
Aoah	13.1	103.7	2.9	6.6	-1.4	0.0293	0.19
C1qtnf3	277.4	2776.8	77.0	219.9	-1.7	0.0003	0.01
Cd74	83.8	2701.3	38.6	355.3	-3.4	0.0000	0.00
Chl1	87.0	560.0	7.3	13.4	-1.1	0.0284	0.19
Chsy1	78.0	715.0	12.2	31.9	-1.6	0.0014	0.02
Col5a1	1136.0	7956.0	88.2	176.3	-1.2	0.0100	0.09
Dmtf1	1.3	50.4	0.2	2.5	-4.0	0.0006	0.01
Dvl3	7.0	70.0	1.5	4.4	-1.7	0.0189	0.14
Efemp2	107.9	666.5	45.2	79.7	-1.0	0.0357	0.22
Epdr1	3.0	181.0	0.8	14.1	-4.3	0.0000	0.00
Esr1	11.5	117.7	1.2	3.5	-1.7	0.0071	0.07
Evc2	7.0	119.0	1.1	5.4	-2.5	0.0003	0.01
Farp1	18.0	194.0	2.4	7.4	-1.8	0.0016	0.02
Fbn2	77.0	922.0	4.8	16.4	-2.0	0.0001	0.00
Foxc1	0.0	41.0	0.0	1.9	-7.8	0.0001	0.00
Frs2	28.0	189.0	3.2	6.2	-1.2	0.0372	0.22
Get4	7.5	72.2	2.3	6.4	-1.6	0.0315	0.20
Gxylt2	4.0	99.0	1.4	10.1	-3.0	0.0001	0.00
Hs2st1	59.0	457.0	8.0	17.7	-1.3	0.0075	0.07
Itga11	25.0	203.0	3.3	7.7	-1.4	0.0110	0.09
Jarid2	0.4	68.1	0.0	2.2	-8.5	0.0000	0.00
Kdelc2	48.0	345.0	8.6	17.6	-1.2	0.0165	0.13
Lgr4	18.0	182.0	2.3	6.7	-1.7	0.0029	0.03
Lpar1	23.9	267.5	4.6	14.8	-1.9	0.0007	0.01
Lrrn4cl	21.0	152.0	5.3	11.0	-1.3	0.0329	0.21
Mgat3	10.0	160.0	1.4	6.4	-2.4	0.0001	0.00
P2rx7	6.4	56.5	1.6	4.1	-1.6	0.0361	0.22
Pde4a	8.3	72.6	1.2	2.9	-1.6	0.0271	0.18
Pik3ip1	8.0	94.0	2.3	7.8	-1.9	0.0045	0.05
Postn	314.0	3045.3	63.7	176.4	-1.7	0.0005	0.01
Prrx1	30.7	213.7	4.0	8.0	-1.2	0.0292	0.19
Ptprd	7.0	139.0	0.5	2.8	-2.7	0.0001	0.00
Ptprj	93.4	655.6	8.0	16.0	-1.2	0.0139	0.11
Rbl2	16.5	189.6	2.2	7.2	-1.9	0.0012	0.02
Rhot1	0.0	65.6	0.0	3.0	-8.5	0.0000	0.00
Rspo3	1.0	35.0	0.3	2.7	-3.4	0.0034	0.04
Senp3	12.0	114.2	3.2	8.7	-1.6	0.0090	0.08
Shc1	4.5	81.7	0.9	4.8	-2.4	0.0013	0.02
Sirt1	4.7	75.7	0.8	3.6	-2.3	0.0026	0.03
Ski	85.0	627.0	10.1	21.4	-1.3	0.0100	0.09
Smoc1	1.2	44.3	0.2	2.4	-3.8	0.0007	0.01
Tanc2	47.0	377.0	2.6	5.9	-1.4	0.0071	0.07
Tgfbr2	110.3	921.3	15.0	35.8	-1.5	0.0029	0.03
Tmem131	66.0	450.0	6.6	12.8	-1.2	0.0199	0.15
Tnfaip8	9.7	142.7	1.9	7.9	-2.2	0.0005	0.01
Trp53inp1	12.8	133.9	1.5	4.6	-1.8	0.0046	0.05
Ubp1	1.4	77.2	0.2	3.7	-4.6	0.0000	0.00
Wnk1	30.0	199.6	1.9	3.5	-1.1	0.0370	0.22
Zcchc14	78.0	729.0	7.9	21.0	-1.6	0.0012	0.02
Zfhx3	27.0	214.0	1.1	2.4	-1.4	0.0116	0.10
Zfhx4	24.0	398.0	1.1	5.3	-2.4	0.0000	0.00

Supplementary Table S2. Significantly downregulated genes in A375/211 xenografts predicted to be MIR211 targets in the mouse.

A375/211 vs. A375		A375/211 vs. A375/211/PDK4		A375/211/PDK4 vs. A375	
Ingenuity Canonical Pathways	**Z-score**	**Ingenuity Canonical Pathways**	**Z-score**	**Ingenuity Canonical Pathways**	**Z-score**
Antioxidant Action of Vitamin C	nd	Antioxidant Action of Vitamin C	nd	Antioxidant Action of Vitamin C	2.000
BMP signaling pathway	nd	BMP signaling pathway	nd	BMP signaling pathway	-2.236
cAMP-mediated signaling	-2.000	cAMP-mediated signaling	-2.111	cAMP-mediated signaling	-1.000
Cardiac Hypertrophy Signaling	-0.333	Cardiac Hypertrophy Signaling	-2.309	Cardiac Hypertrophy Signaling	0.000
Colorectal Cancer Metastasis Signaling	0.218	Colorectal Cancer Metastasis Signaling	-2.132	Colorectal Cancer Metastasis Signaling	0.000
Corticotropin Releasing Hormone Signaling	0.000	Corticotropin Releasing Hormone Signaling	-2.000	Corticotropin Releasing Hormone Signaling	nd
CREB Signaling in Neurons	0.707	CREB Signaling in Neurons	-2.121	CREB Signaling in Neurons	-0.707
Cyclins and Cell Cycle Regulation	2.000	Cyclins and Cell Cycle Regulation	nd	Cyclins and Cell Cycle Regulation	nd
Dopamine-DARPP32 Feedback in cAMP Signaling	-1.508	Dopamine-DARPP32 Feedback in cAMP Signaling	-2.236	Dopamine-DARPP32 Feedback in cAMP Signaling	-1.134
EIF2 Signaling	-0.816	EIF2 Signaling	-2.333	EIF2 Signaling	0.333
eNOS Signaling	-1.732	eNOS Signaling	-2.138	eNOS Signaling	-0.302
ERK5 Signaling	2.236	ERK5 Signaling	0.000	ERK5 Signaling	nd
Gαi Signaling	-2.121	Gαi Signaling	-1.633	Gαi Signaling	nd
Gαq Signaling	-2.333	Gαq Signaling	-2.309	Gαq Signaling	-0.577
Hypoxia Signaling in the Cardiovascular System	2.000	Hypoxia Signaling in the Cardiovascular System	nd	Hypoxia Signaling in the Cardiovascular System	nd
Interferon Signaling	-2.449	Interferon Signaling	-2.449	Interferon Signaling	nd
P2Y Purigenic Receptor Signaling Pathway	0.000	P2Y Purigenic Receptor Signaling Pathway	-2.333	P2Y Purigenic Receptor Signaling Pathway	0.000
PPARα/RXRα Activation	-2.121	PPARα/RXRα Activation	-1.265	PPARα/RXRα Activation	1.342
Relaxin Signaling	-0.816	Relaxin Signaling	-2.121	Relaxin Signaling	-0.378
RhoGDI Signaling	1.000	RhoGDI Signaling	1.508	RhoGDI Signaling	-2.714
Role of NFAT in Regulation of the Immune Response	-1.000	Role of NFAT in Regulation of the Immune Response	-2.111	Role of NFAT in Regulation of the Immune Response	-0.632
SAPK/JNK Signaling	0.000	SAPK/JNK Signaling	-2.449	SAPK/JNK Signaling	0.447
Sperm Motility	-0.378	Sperm Motility	0.000	Sperm Motility	-2.333
Synaptic Long-Term Depression	-0.707	Synaptic Long-Term Depression	nd	Synaptic Long-Term Depression	-2.646
Telomerase Signaling	2.121	Telomerase Signaling	0.000	Telomerase Signaling	0.000

Supplementary Table S3. Ingenuity pathway analysis (IPA) of differential gene expression in A375 xenografts, MIR211-overexpressing xenografts, or MIR211/PDK4 co-expressing xenografts. Turquoise = activated; brown = inactivated. The activation z-score measures the match between expected relationship direction and observed gene expression (≥2 is considered significant).

Gene Set Name	k/K	*p*-value	FDR
EPITHELIAL_MESENCHYMAL_TRANSITION	0.14	9.74E-29	4.87E-27
HYPOXIA	0.13	1.64E-24	4.09E-23
MTORC1_SIGNALING	0.12	8.44E-22	1.41E-20
GLYCOLYSIS	0.10	1.19E-16	1.49E-15
APOPTOSIS	0.09	4.40E-12	4.40E-11
TNFA_SIGNALING_VIA_NFKB	0.08	6.40E-12	5.33E-11
KRAS_SIGNALING_UP	0.06	1.06E-08	6.64E-08
MITOTIC_SPINDLE	0.06	1.06E-08	6.64E-08
P53_PATHWAY	0.06	1.06E-07	5.91E-07
ANGIOGENESIS	0.17	1.26E-07	6.32E-07
HALLMARK_UV_RESPONSE_DN	0.06	5.31E-07	2.41E-06
CHOLESTEROL_HOMEOSTASIS	0.09	6.10E-07	2.54E-06
G2M_CHECKPOINT	0.05	9.69E-07	3.46E-06
INFLAMMATORY_RESPONSE	0.05	9.69E-07	3.46E-06
SPERMATOGENESIS	0.06	3.41E-06	1.14E-05
E2F_TARGETS	0.05	7.98E-06	2.35E-05
IL2_STAT5_SIGNALING	0.05	7.98E-06	2.35E-05
ADIPOGENESIS	0.04	5.88E-05	1.63E-04
PI3K_AKT_MTOR_SIGNALING	0.06	7.15E-05	1.88E-04
FATTY_ACID_METABOLISM	0.04	9.03E-05	2.15E-04
UV_RESPONSE_UP	0.04	9.03E-05	2.15E-04
ESTROGEN_RESPONSE_LATE	0.04	3.83E-04	8.33E-04
MYC_TARGETS_V1	0.04	3.83E-04	8.33E-04
TGF_BETA_SIGNALING	0.07	4.46E-04	9.30E-04
ANDROGEN_RESPONSE	0.05	5.61E-04	1.12E-03
APICAL_JUNCTION	0.03	2.18E-03	3.76E-03
COMPLEMENT	0.03	2.18E-03	3.76E-03
MYOGENESIS	0.03	2.18E-03	3.76E-03
XENOBIOTIC_METABOLISM	0.03	2.18E-03	3.76E-03
COAGULATION	0.04	2.26E-03	3.76E-03
PROTEIN_SECRETION	0.04	3.78E-03	6.10E-03
BILE_ACID_METABOLISM	0.04	6.52E-03	1.02E-02
ALLOGRAFT_REJECTION	0.03	1.06E-02	1.52E-02
ESTROGEN_RESPONSE_EARLY	0.03	1.06E-02	1.52E-02
HEME_METABOLISM	0.03	1.06E-02	1.52E-02
PEROXISOME	0.03	3.15E-02	4.37E-02

Supplementary Table S4. Gene set enrichment analysis of differentially expressed genes in MIR211-overexpressing A375 melanoma xenografts

Genomic Region[a]	Refseq	Gene	Peak ID[b]	length	p-value	Fold Enrichment[c]	q-value
chr17:41843518-41843600	NM_004090	DUSP3	S23_peak_6881	172	9.76E-11	4.6	6.75E-07
chr17:41843600-41843689	NM_004090	DUSP3	S21_peak_5357	90	4.53E-06	2.8	0.009936
chr17:41845784-41845786	NM_004090	DUSP3	S21_peak_5358	108	4.98E-06	2.2	0.010662
chr17:41843753-41843833	NM_004090	DUSP3	S23_peak_6882	81	3.27E-05	2.3	0.041924
chr17:41845786-41845829	NM_004090	DUSP3	S23_peak_6883	106	1.78E-13	3.8	2.55E-09
chr8:29192622-29192688	NM_001394	DUSP4	S23_peak_14673	67	2.47E-05	1.8	0.032562
chr8:29193805-29193863	NM_001394	DUSP4	S23_peak_14674	59	1.08E-05	1.9	0.015964
chr8:29197663-29197726	NM_001394	DUSP4	S23_peak_14675	64	1.70E-06	2.4	0.003438
chr12:89743111-89743112	NM_001946	DUSP6	S21_peak_3124	56	2.35E-05	1.9	0.03739
chr12:89743166-89743175	NM_001946	DUSP6	S23_peak_3976	64	3.70E-05	1.8	0.046672
chr12:89745439-89745633	NM_001946	DUSP6	S21_peak_3125	195	5.60E-12	4.6	6.97E-08
chr12:89745908-89746077	NM_001946	DUSP6	S23_peak_3977	170	3.45E-07	3.4	0.000881
chr2:183962890-183962950	NM_080876	DUSP19	S21_peak_7263	61	2.22E-07	5.1	0.000726
chr11:102220458-102220491	NM_001166	BIRC2	S21_peak_2502	55	4.98E-06	2.2	0.010662
chr11:102220491-102220512	NM_001166	BIRC2	S21_peak_2502	55	4.98E-06	2.2	0.010662
chr11:102221400-102221459	NM_001166	BIRC2	S21_peak_2503	60	3.34E-11	6.6	3.48E-07

Supplementary Table S5. The enrichment of *BIRC2* and DUSPs RNAs by Ago2-immunopurification

[a] hg19 genomic coordination

[b] S21 and S23 are two independent RIP-seq replicates.

[C] Fold enrichment compared to input.

MIR211 low expressors					MIR211 high expressors				
Cell line	MIR211 Ct	RNU48 Ct	-ΔCt	AUC vemurafenib resistance	Cell line	MIR211 Ct	RNU48 Ct	-ΔCt	AUC vemurafenib resistance
UACC-1097	38.4	22.9	-15.44	1.05	UACC-2994	27.8	21.6	-6.16	1.08
UACC-3291	38.3	22.9	-15.41	0.49	UACC-0903	28.6	23.1	-5.47	0.50
UACC-0558	38.4	23.0	-15.37	0.72	SK-MEL-119	27.9	22.5	-5.41	1.14
A375	38.1	23.1	-15.08	0.50	SK-MEL-217	27.2	22.1	-5.08	1.05
UACC-0502	38.3	23.4	-14.94	0.68	UACC-3312	25.3	21.9	-3.44	1.06
UACC-3337	37.3	22.7	-14.63	1.01	SK-MEL-113	25.4	22.3	-3.07	1.15
UACC-2331	36.8	22.6	-14.25	0.82	UACC-1649	25.9	23.0	-2.88	1.12
UACC-1118	37.3	23.4	-13.91	1.08	UACC-0257	25.3	22.6	-2.67	0.67
SK-MEL-2	36.6	22.9	-13.71	1.04	UACC-2427	27.7	25.7	-1.99	1.05
UACC-1237	35.9	22.2	-13.64	0.81	UACC-1120	24.0	22.1	-1.92	0.65
UACC-2641	35.3	22.3	-12.99	0.95	MeWo	24.2	22.5	-1.69	1.09
UACC-1729	35.9	22.9	-12.97	0.96	UACC-0091	23.7	22.8	-0.96	0.73
UACC-1113	35.3	22.4	-12.86	1.03	UACC-2972	22.9	22.1	-0.83	1.24
UACC-0612	35.4	22.6	-12.83	0.93	UACC-1308	23.0	22.6	-0.38	0.48
UACC-0647	35.6	22.9	-12.71	0.99	UACC-1940	25.6	25.5	-0.09	1.20
UACC-3074	34.6	22.1	-12.52	1.05	UACC-3093	24.3	24.4	0.08	1.01
UACC-1093	36.2	23.9	-12.28	0.93	SK-MEL-21	22.2	22.5	0.30	1.22
UACC-0952	34.9	23.3	-11.60	1.01					
UACC-1469	34.7	23.2	-11.55	1.04					
UACC-2496	34.8	23.6	-11.19	0.94					
UACC-2851	33.5	22.9	-10.58	1.00					
UACC-2610	33.1	22.5	-10.55	1.04					

Supplementary Tabel S6. The level of MIR211 expression and vemurafenib resistance of various melanoma cell lines. (-ΔCt = -(Ct of MIR211 – Ct of RNU48) from qRT-PCR)

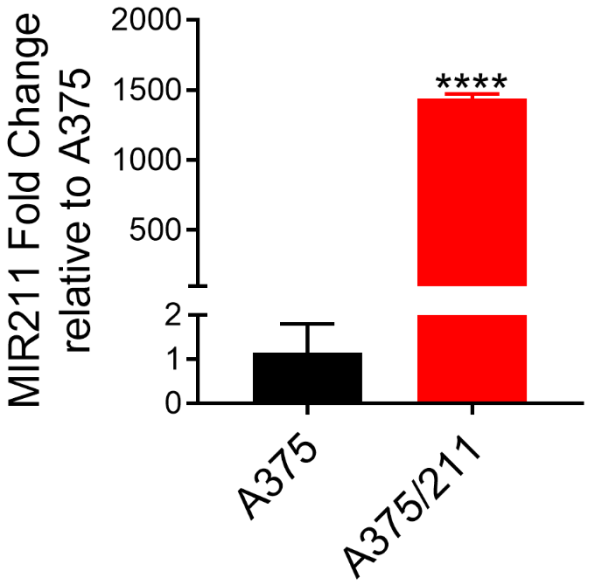

Supplementary Figure S1. qRT-PCR-detected changes in MIR211 in A375 and A375/211 cells. (unpaired student t-test, **** $p \leq 0.0001$)

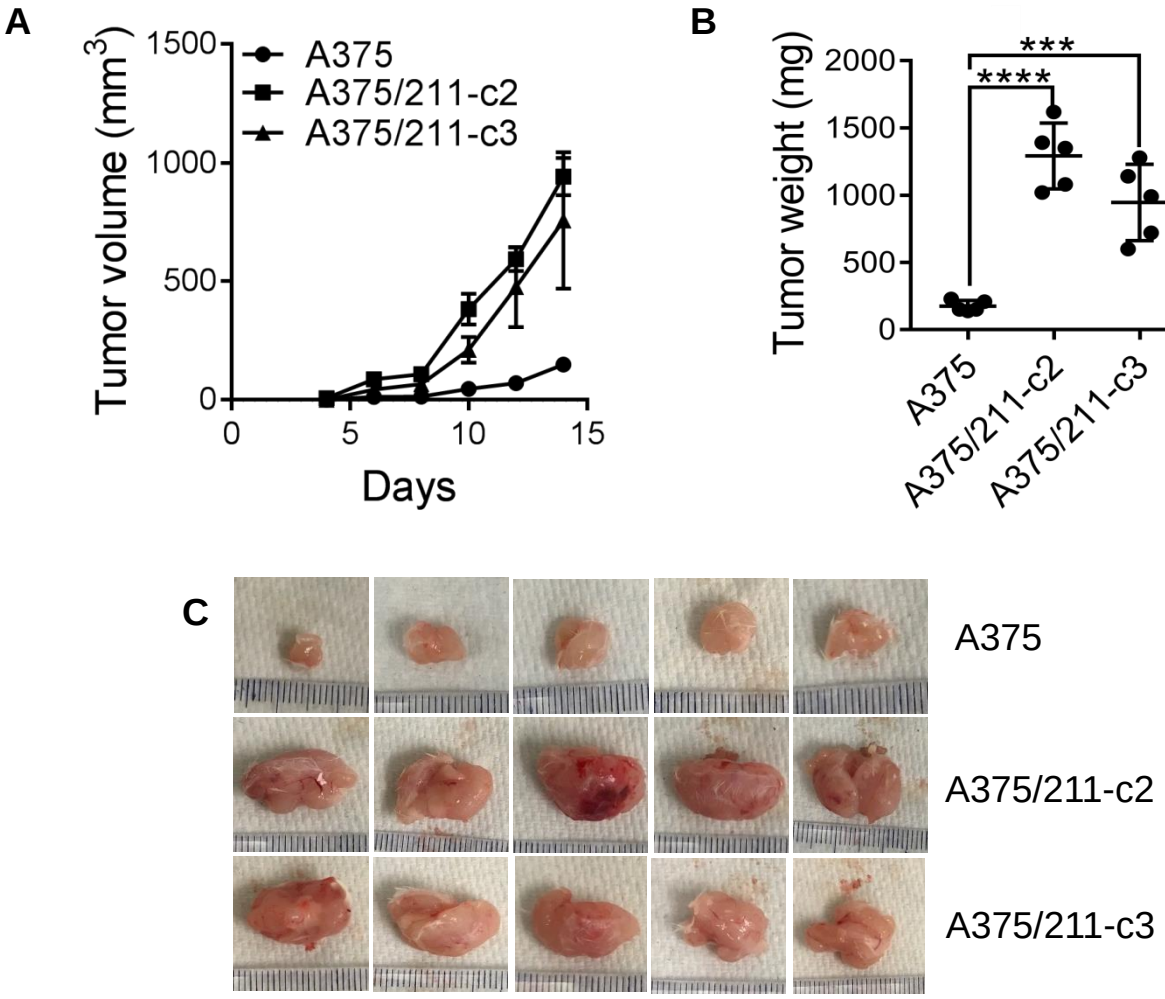

Supplementary Figure S2. Different MIR211-overexpressing A375 clones grown as xenografts *in vivo*.
(A) A375 amelanotic melanoma cells and their MIR211 overexpressing counterparts (A375/211-c2 and -c3) were injected subcutaneously into the flanks of SCID mice and tumor volume measured with electronic calipers until termination of the experiment at 12 days. A375/211 tumors were significantly larger and grew more rapidly than the other tumors.
(B) Tumors were excised and weighed at the termination of the experiment at 12 days. MIR211-overexpressing tumors were significantly heavier than either parental A375 xenografts. (unpaired student t-test, *** $p < 0.001$, *** $p < 0.0001$)
(C) Photographs of subcutaneous tumor xenografts at the termination of the experiment at day 12. MIR211-overepxressing xenografts were larger than parental controls.

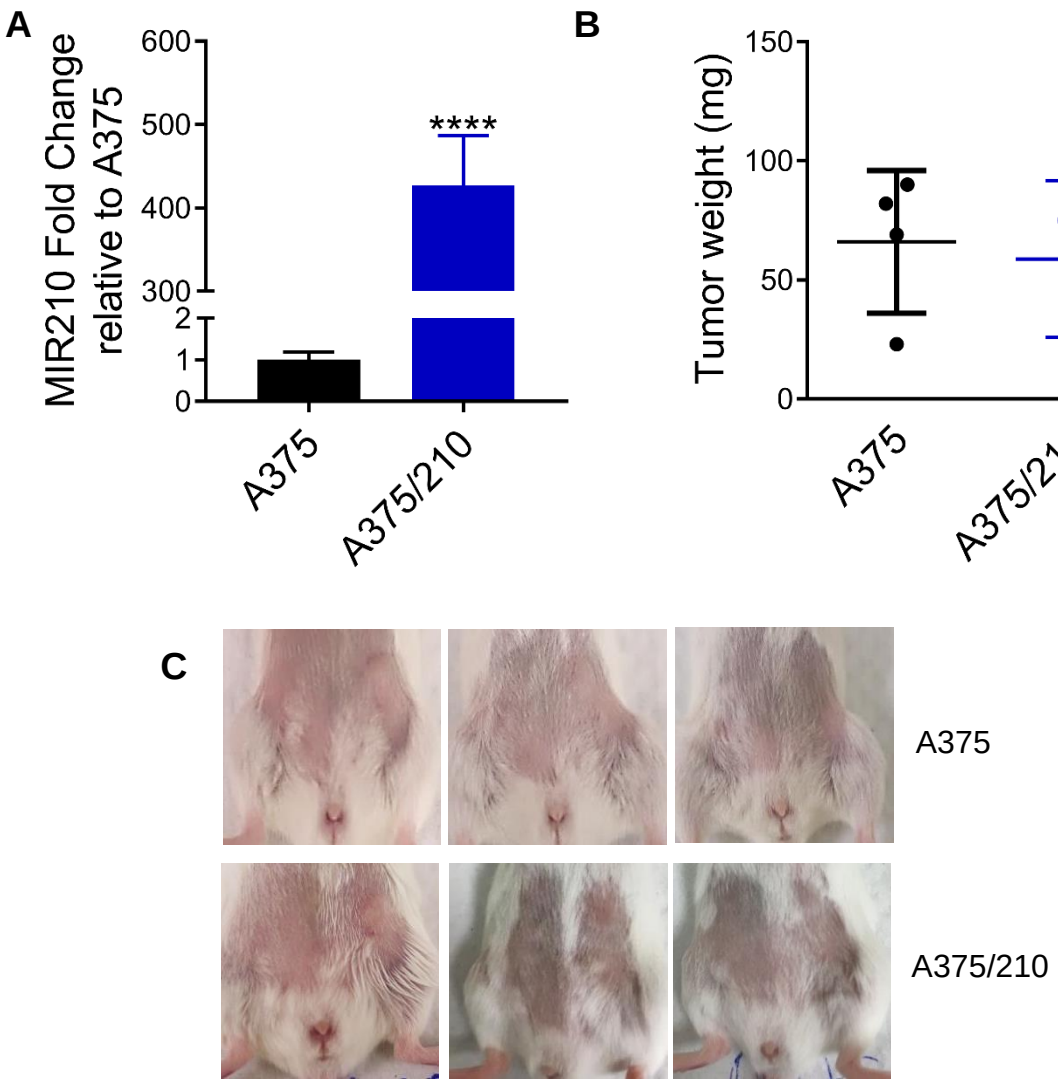

Supplementary Figure S3. (A) qRT-PCR-detected changes in MIR210 in A375 and A375/210 cells (B) Tumors were excised and weighed at the termination of the experiment at 12 days. MIR210-overexpressing tumors were not significantly different to parental A375 xenografts. (unpaired student t-test, **** $p \leq 0.0001$, ns: not significant) (C) Photographs of subcutaneous tumor xenografts at the termination of the experiment at day 12.

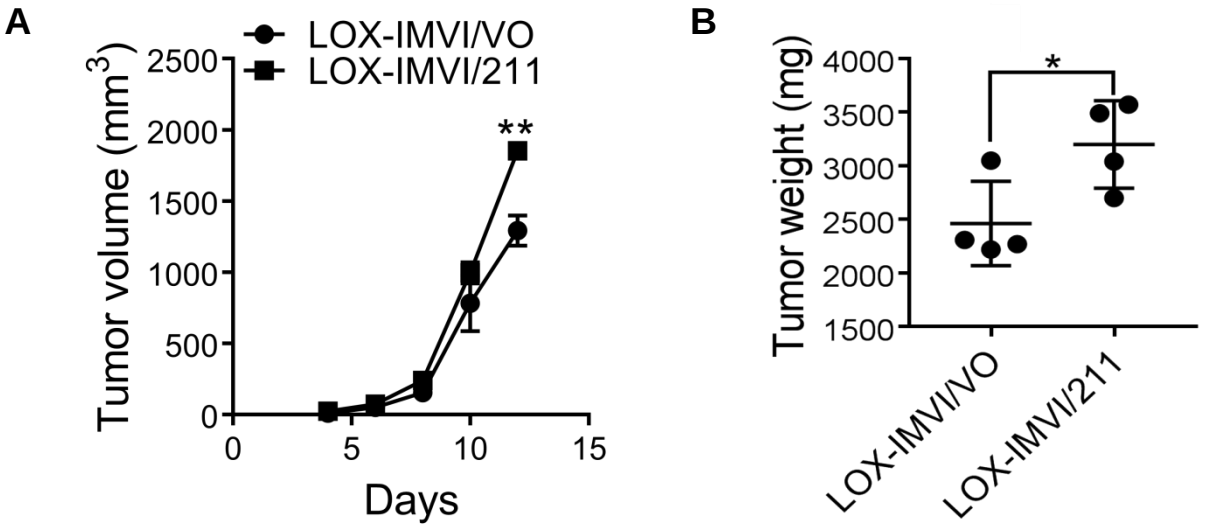

Supplementary Figure S4. Ectopic expression of MIR211 in LOX-IMVI cells increased tumor growth. LOX-IMVI stably expressing MIR211 cells were implanted in the flanks of SCID mice. (A) Tumor size was measured and tumor volume was calculated as described in the Methods. (B) Mice were sacrificed at day 12 and tumors were excised and weighed. (LOX-IMVI/VO: LOX-IMVI with vector only; LOX-IMVI/211: cells expressing MIR211, unpaired student's *t*-test, * $p \leq 0.05$, ** $p \leq 0.01$)

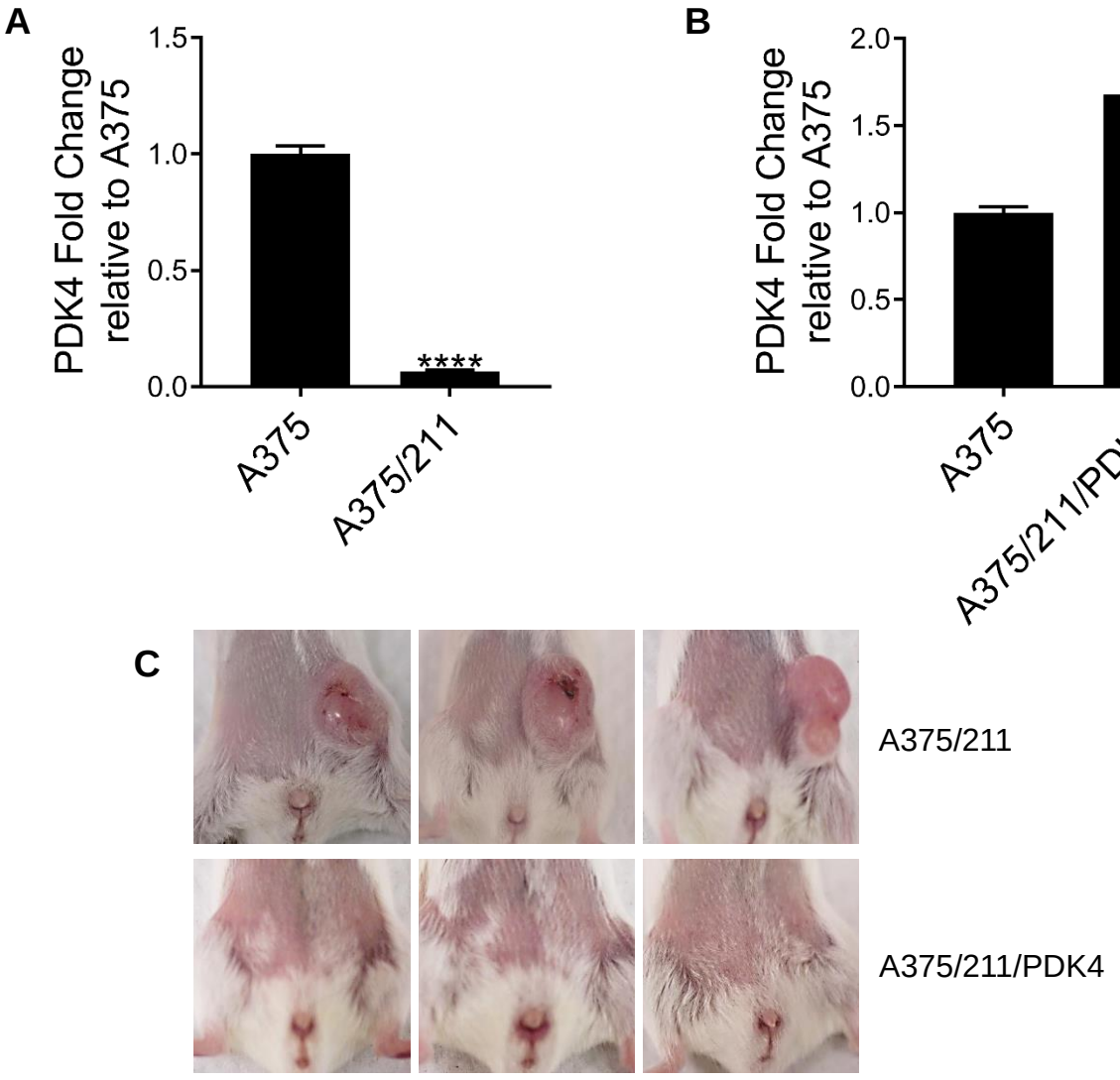

Supplementary Figure S5. qRT-PCR-detected changes in PDK4 (A) in A375 and A375/211 cells (B) in A375 and A375/211/PDK4 cells. (unpaired student t-test, ** $p \leq 0.01$ **** $p \leq 0.0001$)
(C) Photographs of subcutaneous tumor xenografts at the termination of the experiment at day 12. The PDK4 expression in A375/211 reduced the tumor growth.

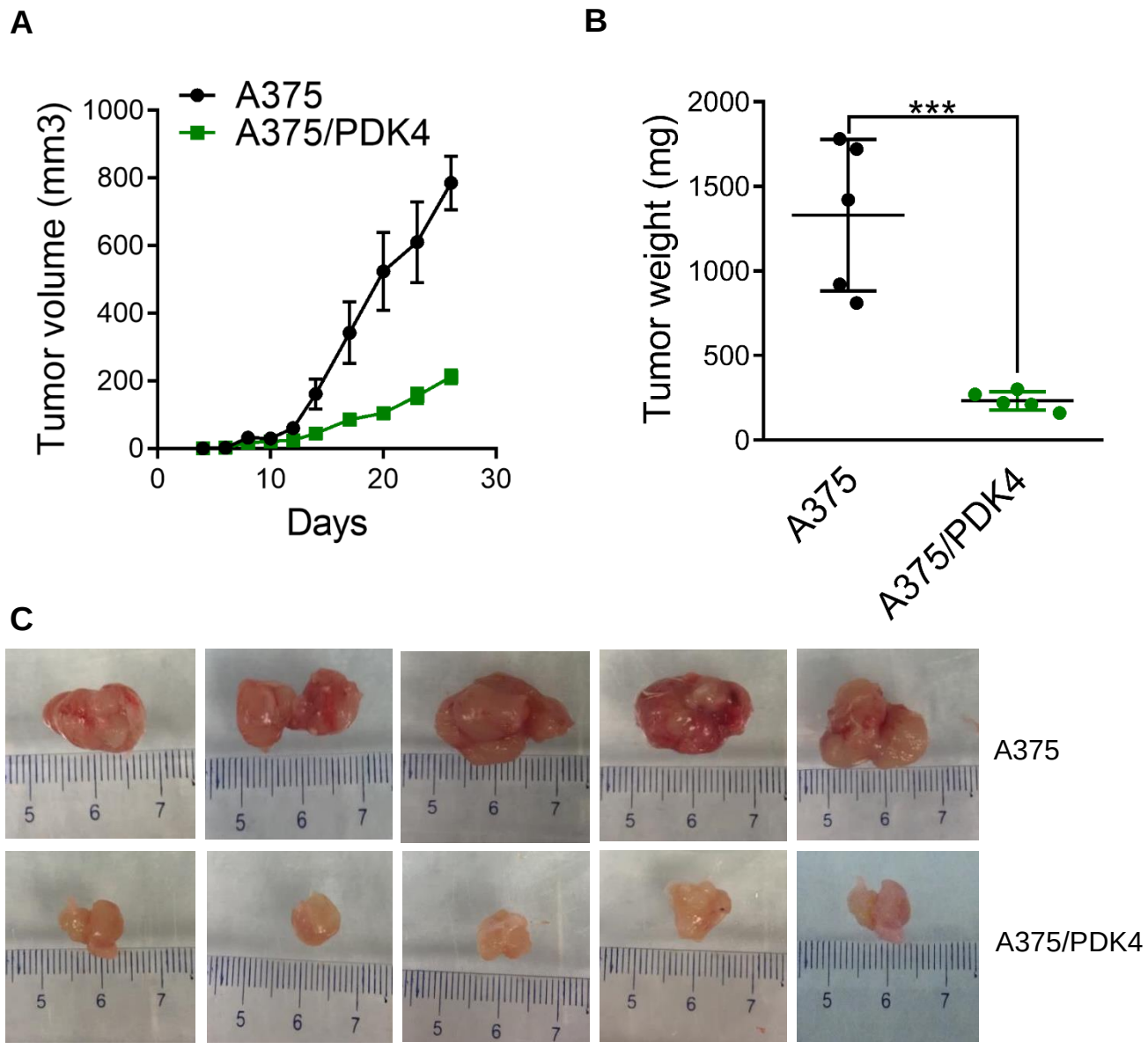

Supplementary Figure S6. Ectopic expression of PDK4 reduces tumor growth *in vivo*.
(A) A375 melanoma cells and their PDK4 overexpressing counterparts (A375/PDK4) were injected subcutaneously into the flanks of SCID mice and tumor volume measured with electronic calipers until termination of the experiment at 26 days. A375/PDK4 tumors were significantly smaller and grew more slowly than the other tumors. (student t-test, * $p < 0.05$, ** $p < 0.01$, *** $p < 0.001$)
(B) Tumors were excised and weighed at the termination of the experiment at 26 days. PDK4-overexpressing tumors were significantly lighter than either parental A375 xenografts. (*** $p < 0.001$)
(C) Photographs of subcutaneous tumor xenografts at the termination of the experiment at day 26. PDK4 overepxressing xenografts were smaller than parental controls.

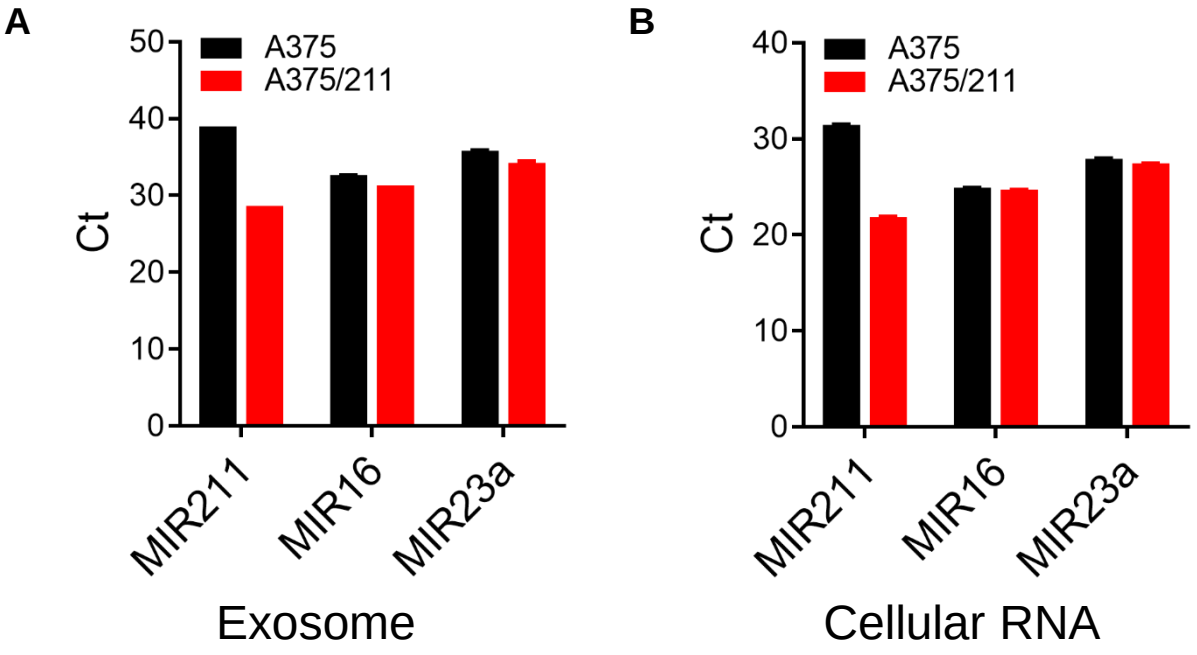

C

hsa-MIR-211 5′–UUCCCUUUGUCAUCCUUCGCCU–3′

mmu-Mir-211 5′–UUCCCUUUGUCAUCCUUUGCCU–3′

Supplementary Figure S7. qRT-PCR showing detection of MIR211, MIR16, and MIR23a (A) in exosomes and (B) cellular RNAs. (C) Differences between the human and mouse MIR211 sequences.

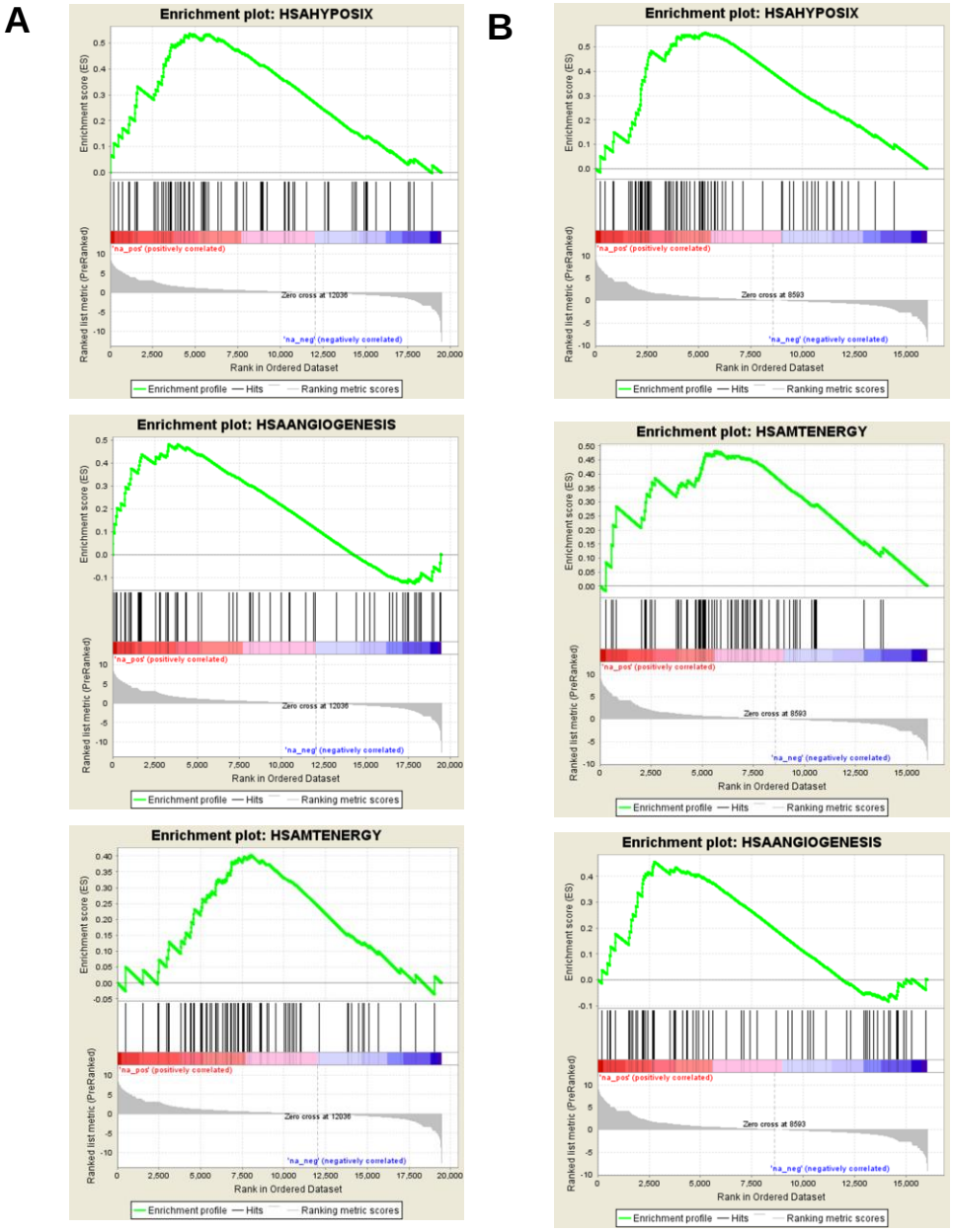

Supplementary Figure S8. Gene Set Enrichment Analysis (GSEA) of differentially expressed human (A) and mouse (B) genes in A375/211 vs. A375 xenografts. Hypoxia and angiogenesis pathways were significantly enriched in both human and mouse cells. Mitochondrial Energy metabolism pathways were enriched, but not significantly.

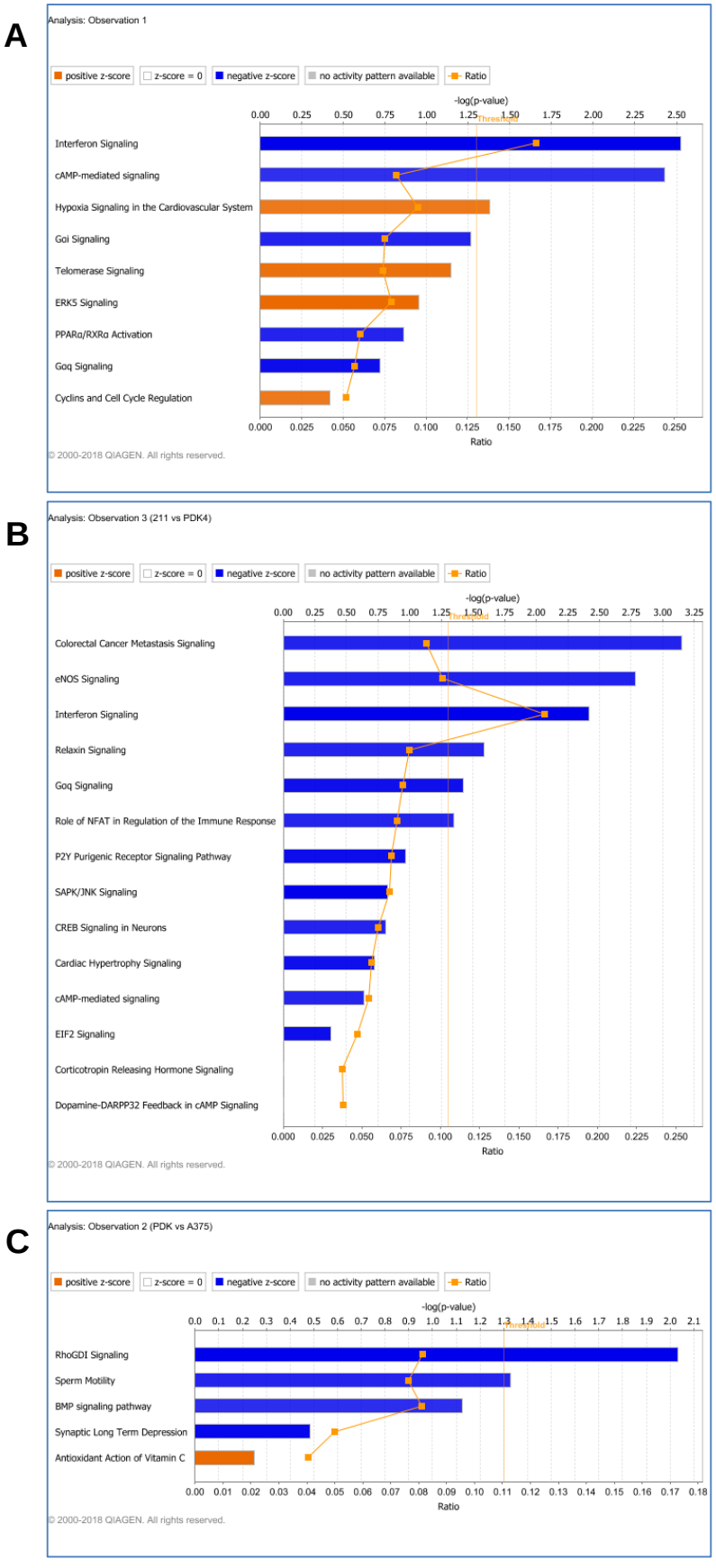

Supplementary Figure S9. Canonical Ingenuity Pathway Analysis (IPA) of differential gene expression in (A) A375 vs A375/211 (B) A375/211 vs A375/211/PDK4 and (C) A375/211/PDK vs A375 xenografts.

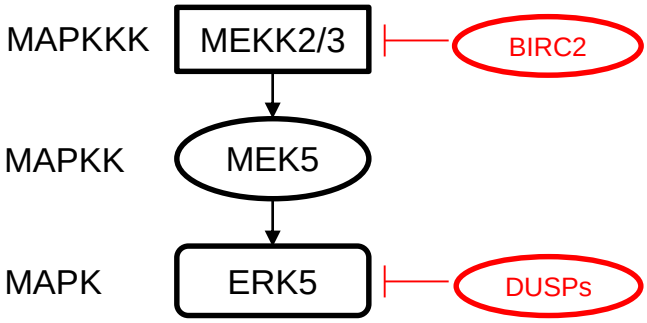

Supplementary Figure S10. Schematic diagram of ERK5 pathway. BIRC2 and DUSPs are putative MIR211 targets that negatively regulate ERK5 signaling. BIRC2 inhibits MEKK2/3 by ubiquitination. DUSPs inhibits ERK5 by dephosphorylation.

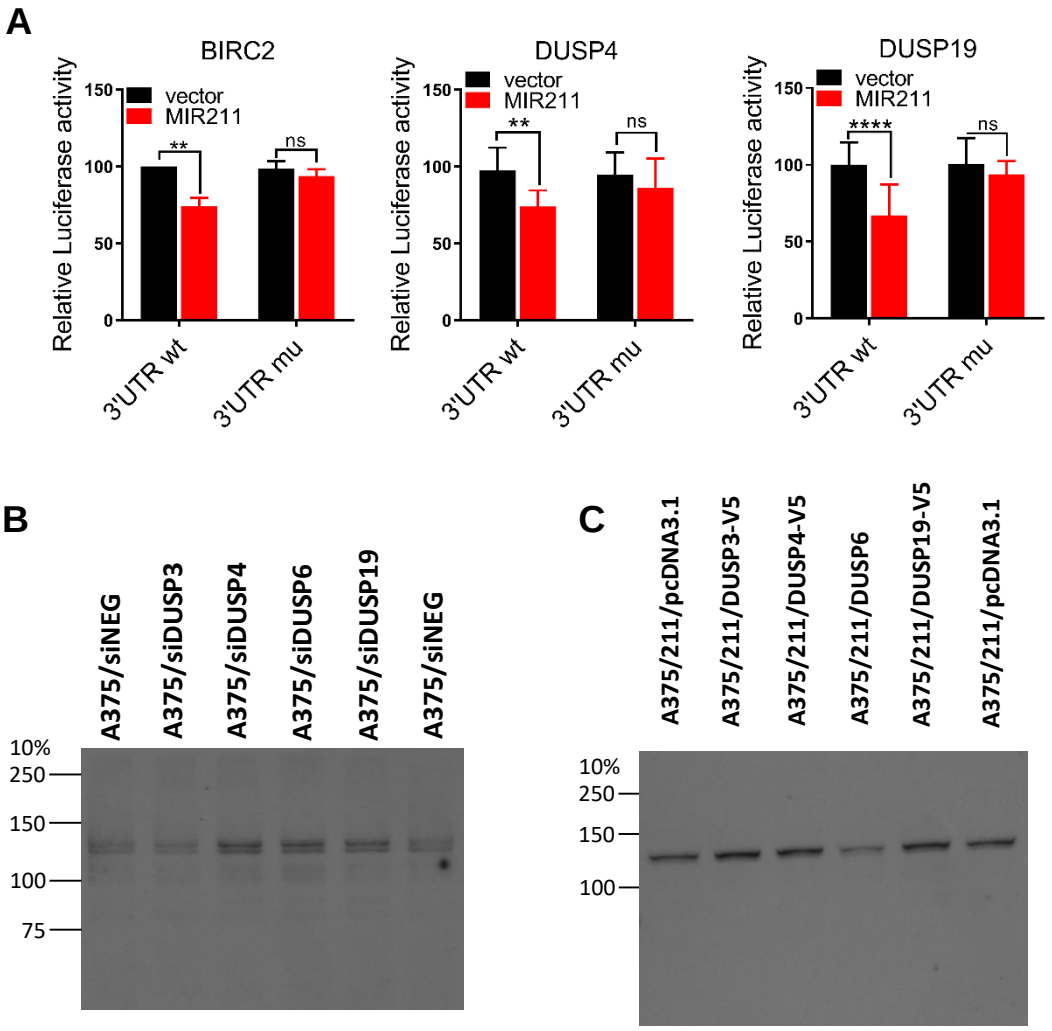

Supplementary Figure S11

A. Luciferase reporter assays carrying either wild-type 3'UTR or a mutant with several nucleotides swapped in the region corresponding to the MIR211 seed. When reporter plasmids were co-transfected with plasmids expressing MIR211 into HEK-293T cells, the wild-type BIRC2, DUSP4, and DUSP19 reporters showed reduced luciferase activity, while the mutant one did not. (Student t-test, ns: not significant, ** $p \leq 0.05$, **** $p \leq 0.0001$)

B. phosphor-ERK5 detection by western blot analysis of A375 cells transiently transfected with DUSPs siRNAs.

C. phosphor-ERK5 detection by western blot analysis of A375/211 cells transiently transfected with plasmids harboring each DUSP gene.

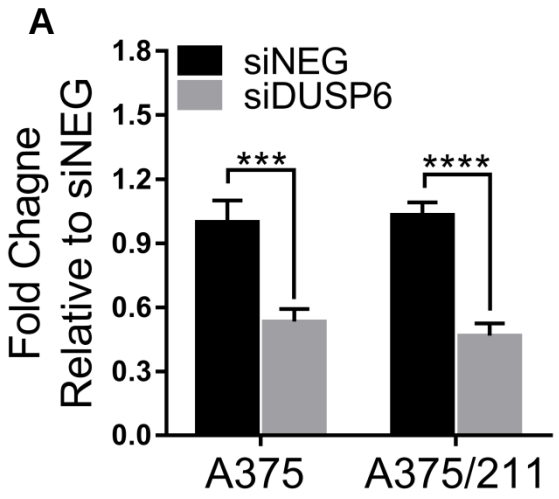

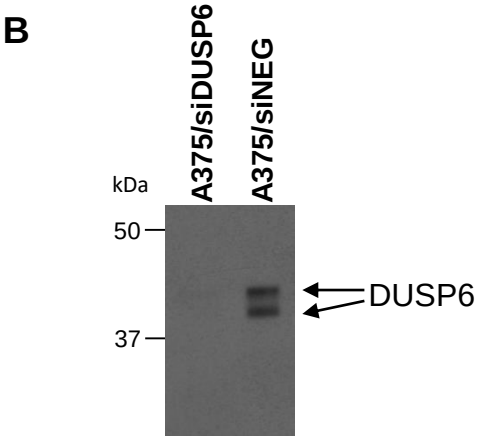

Supplementary Figure S12. qRT-PCR (A) and western blot (B) confirmation of DUSP6 knockdown by siRNA.

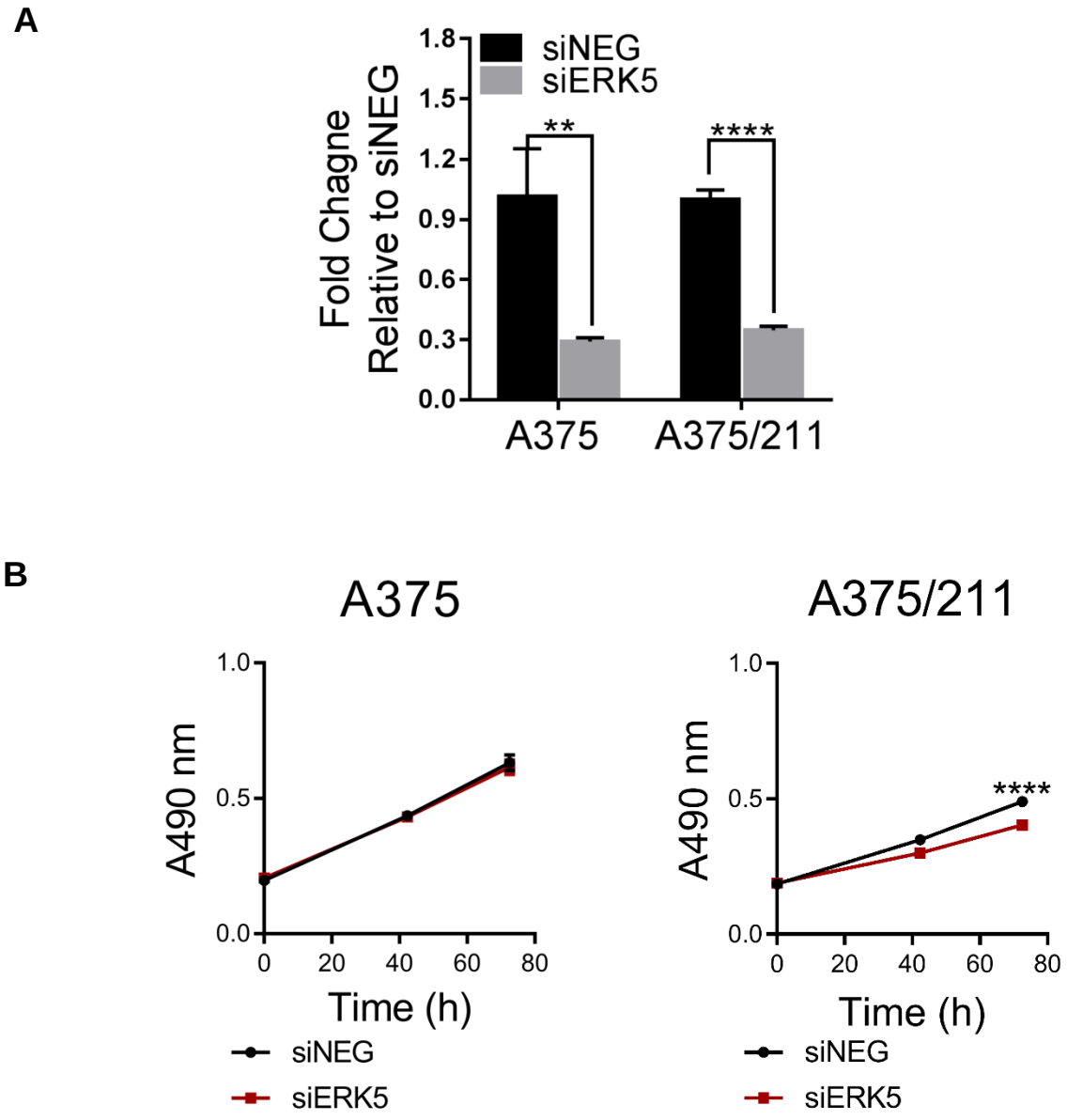

Supplementary Figure S13. (A) qRT-PCR confirmation of ERK5 knockdown by siRNA. (B) ERK5 knockdown by siRNA reduced cell viability in A375/211 cells but not A375 cells. (unpaired student t-test, **** $p \leq 0.0001$)

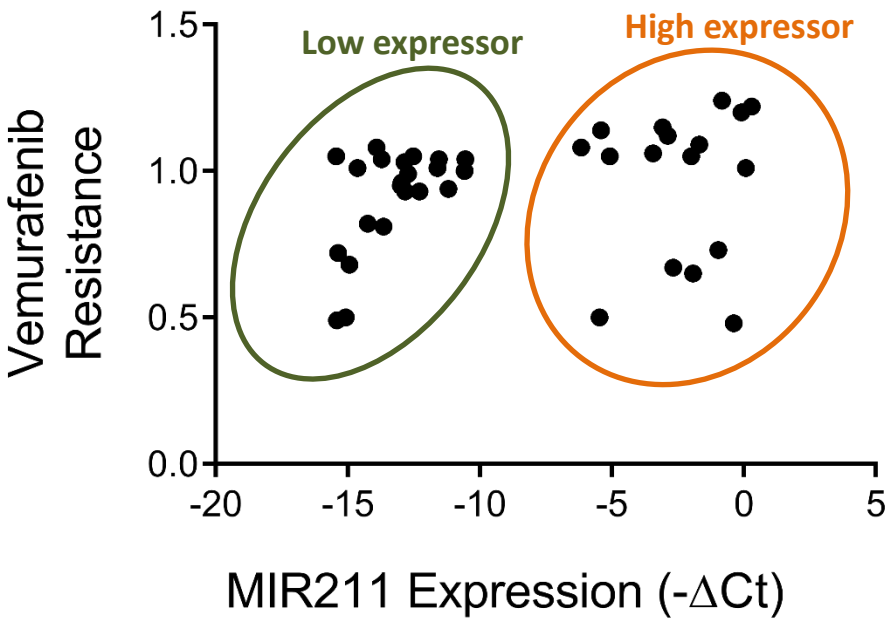

Supplementary Figure S14. The level of MIR211 expression and vemurafenib resistance distinguished melanoma cell lines into two groups, MIR211 low expressors and high expressors. Low expressors showed the correlation between MIR211 expression and vemurafenib resistance, while high expressors did not.

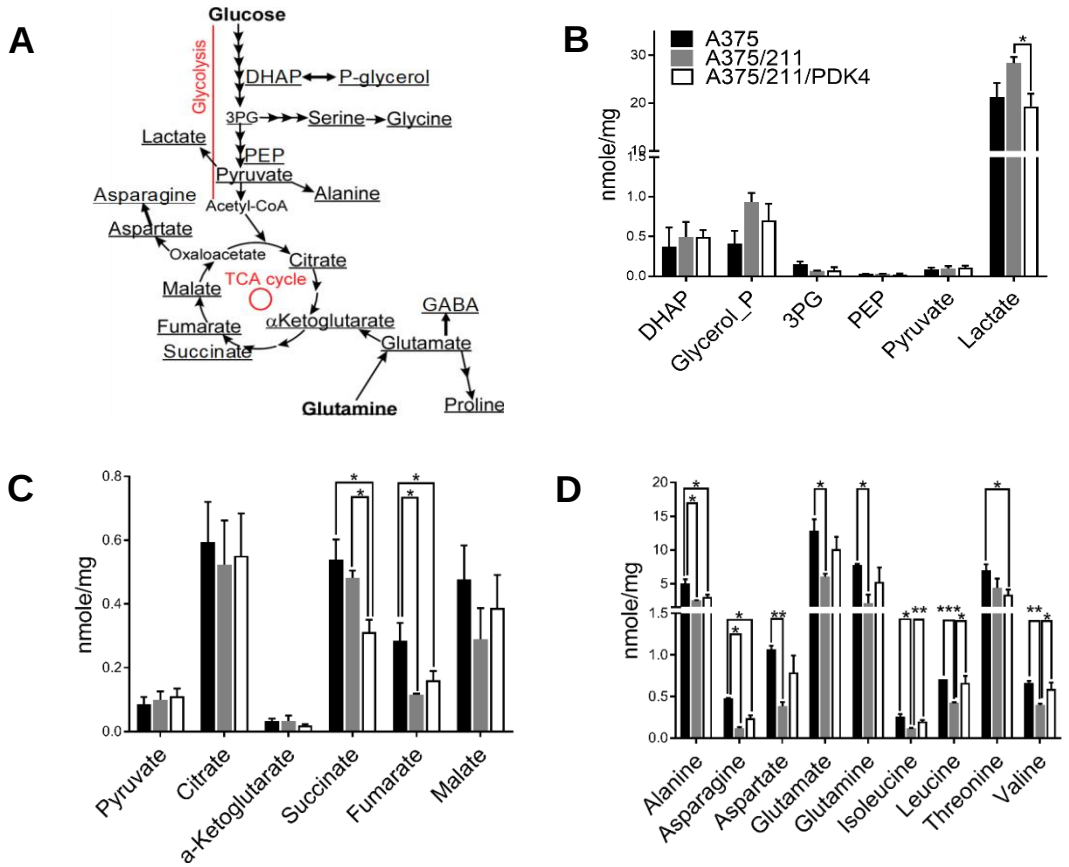

Supplementary Figure S15. Targeted metabolomic analysis of A375/211 xenografts.
(A) Schematic of the glycolytic and tricarboxylic cycle (TCA) pathways.
(B-D) *In vivo* targeted metabolomics of (B) glycolysis and glycolytic intermediates, (C) the TCA cycle, and (D) amino acids of A375 (black bars), A375/211 (gray bars), and A375/211/PDK4 (white bars) xenografts. (unpaired student t-test, ** $p \leq 0.05$; ** $p \leq 0.01$, *** $p \leq 0.001$)